

# Carbon Nanotube DNA Sensor and Sensing Mechanism

Xiaowu Tang,<sup>\*,†,‡</sup> Sarunya Bansaruntip,<sup>‡</sup> Nozomi Nakayama,<sup>‡</sup> Erhan Yenilmez,<sup>‡</sup> Ying-lan Chang,<sup>§</sup> and Qian Wang<sup>‡</sup>

*Department of Chemistry, University of Waterloo, Waterloo, Ontario N2L 3G1, Canada, Department of Chemistry, Stanford University, Stanford, California 94305, and Agilent Laboratories, Agilent Technologies, Inc., Palo Alto, California 94304*

Received March 18, 2006; Revised Manuscript Received June 7, 2006

## ABSTRACT

We report the fabrication of single-walled carbon nanotube (SWNT) DNA sensors and the sensing mechanism. The simple and generic protocol for label-free detection of DNA hybridization is demonstrated with random sequence 15mer and 30mer oligonucleotides. DNA hybridization on gold electrodes, instead of on SWNT sidewalls, is mainly responsible for the acute electrical conductance change due to the modulation of energy level alignment between SWNT and gold contact. This work provides concrete experimental evidence on the effect of SWNT–DNA binding on DNA functionality, which will help to pave the way for future designing of SWNT biocomplexes for applications in biotechnology in general and also DNA-assisted nanotube manipulation techniques.

The development of electrochemical DNA sensors with high potential for miniaturization and integration has become a subject of intense research, with the hope to make sophisticated and challenging molecular diagnostics available for low-cost routine clinical practice. Electronic detection methods based on electrodes,<sup>1,2</sup> CMOS field effect transistor (FET),<sup>3–5</sup> and the more recent nanowire/nanotube (NW/NT) DNA sensors<sup>6,7</sup> have been reported, which have shown great promise in higher sensitivity and large scale arrayability. The extreme sensitivity of NW and NT field-effect sensors originates from their one-dimensional structure that enables efficient charge transfer between the surface-anchored DNAs and NW/NT. However, they are also highly sensitive to impurities and other ionic species in analyte solution, especially at the acclaimed low DNA concentration. As a result, low ionic strength buffer is quite often necessary,<sup>7</sup> and studies on sensing mechanism are proven to be difficult. Newly reported research on SWNT-FET based gas,<sup>8,9</sup> protein,<sup>10</sup> and DNA<sup>6</sup> sensors has indicated that the sensing mechanism differs significantly when applied to different analyte molecules despite the commonality among the devices themselves. While learning from our previous studies on protein sensing,<sup>10</sup> it is of vital importance to better understand the unique SWNT–DNA interaction and its effect on the inherent affinity of DNA strands and therefore sensing.

Furthermore, a platform that is simple, reliable, and general irrespective of sequence is required for molecular diagnostics. Here, we demonstrate the fabrication of virtually two-terminal SWNT–DNA sensor arrays and the simple and yet generic protocol for direct label-free detection of DNA hybridization in a biocompatible buffer solution. We also carried out a systematic study of sensing mechanism, involving X-ray photoelectron spectroscopy (XPS), quartz crystal microbalance (QCM), and fluorescence measurements.

SWNTs were synthesized by thermal chemical vapor deposition (CVD) on a 4 in. SiO<sub>2</sub> wafer with prepatterned iron film (~10 nm thick). About 100 tubes were grown semiparallel across each pair of closely positioned (5 μm) catalyst islands, upon which metal electrodes (30 nm of Au on top of 0.5 nm of Ti) were deposited. For current study, the 4 in. wafer was made into hundreds of chips (0.75 cm × 0.75 cm), each accommodating four to six SWNT sensory devices (Figure 1a). Each sensor is a field effect device, which has a typical on-current of 3–6 μA at 10 mV source-drain bias and an on–off ratio about 3 due to the presence of both semiconducting (2/3) and metallic (1/3) tubes.

Selectivity and sensitivity of SWNT electronic sensors were demonstrated on two synthetic DNA systems (Stanford Protein and Nuclear Acid Biotechnology Facility) with 15mer and 30mer, respectively. The random sequenced 15mer thiolated ssDNA probe (*p15*), its completely complementary target ssDNA (*CM15*), and its also random generated mismatched target ssDNA (*MM15*) are SH–C<sub>6</sub>–5′–CATTC–CGAGTGTTC–3′, 5′–TGGACACTCGGAATG–3′, and 5′–

\* To whom correspondence may be addressed: Department of Chemistry, University of Waterloo, 200 University Ave. West, Waterloo, ON, Canada N2L 3G1. E-mail: tangxw@uwaterloo.ca. Phone: 519-888-4567 ext. 8037. Fax: 519-746-0435.

† University of Waterloo.

‡ Stanford University.

§ Agilent Laboratories, Agilent Technologies, Inc.

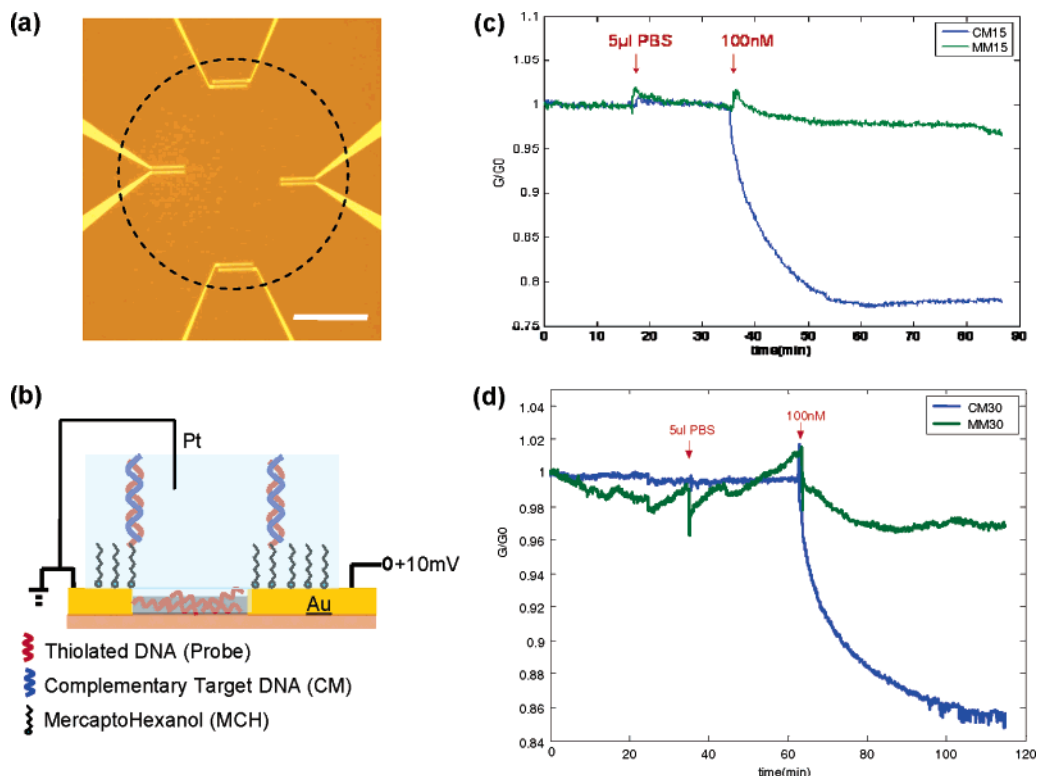


**Figure 1.** (a) Optical image of the central region of a single sensor chip with four SWNT devices (scale bar 200  $\mu\text{m}$ ). Electrodes extending out of the liquid cell (dashed circle) connect to large wire bonding pads. (b) Schematic illustration of a single device during electrical measurement. Complementary ssDNA oligos hybridize to thiolated ssDNA coimmobilized with MCH on the gold electrodes. Real-time monitoring of 15mer (c) and 30mer (d) DNA hybridization in PBS, pH 7.4, is shown. Two liquid cells were used in parallel for simultaneous drop adding 5  $\mu\text{L}$  of complementary and mismatched target oligo solutions to 500  $\mu\text{L}$  of buffer. The conductance of a nanotube device functionalized with thiolated ssDNA exhibits selective response to the addition of complementary ssDNA.

GATCTGAGTATCCGT-3'. The sequences of the 30mer counterparts are SH-C<sub>6</sub>-5'-AGACCTCCAGTCTCCATGT-TACGTCTGAT-AC-3' (*p30*), 5'-GTATCAGACGTAA-CATGGAGACTGGAGTCT-3' (*CM30*), and 5'-ACGCT-GAGTACGGGTGCAAGAGTCAAGACTC-3' (*MM30*). Also acquired from the same source are Cy3 labeled *CM15* and *MM15* for fluorescence measurements.

Prior to electrical measurements, individual chips were pretreated with mercaptohexanol (MCH, Aldrich) by immersing in 10 mM MCH aqueous solution overnight. After rinsing thoroughly with ultrapure deionized water (DUIF water, Fisher Scientific) and dried with a N<sub>2</sub> stream, a sensor chip was then wire bonded, packaged into a 28-pin PLCC socket (Jameco Electronics), and loaded into a homemade static liquid cell. The sensors located in the central region (~4 mm diameter) of the chip (Figure 1a) were exposed to 10  $\mu\text{M}$  thiolated ssDNA (*p15* or *p30*) solution in phosphate-buffered saline (PBS, pH 7.4, Fisher Scientific) for 10 h to allow surface immobilization of capturing probe oligos. The sensory surface, as well as the liquid cell, was then flushed with multicopies of PBS to remove unbond probes. The electrical sensing of DNA hybridization was carried out real time by monitoring the source-drain currents of up to four sensors in response to the addition of complementary and mismatched target ssDNA oligos in PBS, pH 7.4, using a HP 4156B semiconductor parameter analyzer (Agilent Technologies). A platinum (Pt) wire was inserted into the analyte solution as a top gate electrode. A 10 mV source-

drain bias was maintained at all times during electrical measurements, while both the Pt top gate and the silicon backgate were grounded to reduce electrical noise. The electrical conductance of a SWNT device functionalized with MCH and thiol-ssDNA capturing probes, as shown schematically in Figure 1b, exhibits almost no change upon addition of PBS or mismatched ssDNAs (*MM15/MM30*), but significantly decreases (~20%) as response to 100 nM complementary target ssDNAs (*CM15/CM30*) (parts c and d of Figure 2). The electrical response is believed to be a true representation of DNA hybridization kinetics, which is in excellent agreement with literature<sup>11</sup> and our QCM analysis on MCH-coated gold surface (supporting document). The easy to scale-up device fabrication technique, the fast read-out, the biocompatible detection environment, and the simplicity and generality of our label-free detection protocol make SWNT sensor a promising candidate for highly miniaturized gene chip and hand-held diagnostic electronics, which eliminates the need of labor-intensive labeling and sophisticated measurement equipments.

The sensing mechanism suggested previously by Star et al. attributes the electrical conductance change to the electron doping by DNA hybridization on the SWNT sidewall.<sup>6</sup> However, their study did not take into consideration the effect of metal contacts, even though DNA hybridization on gold electrodes was evident in their fluorescence images. It is well accepted that SWNT-FETs operate as unconventional Schottky barrier (SB) transistors, in which switching occurs

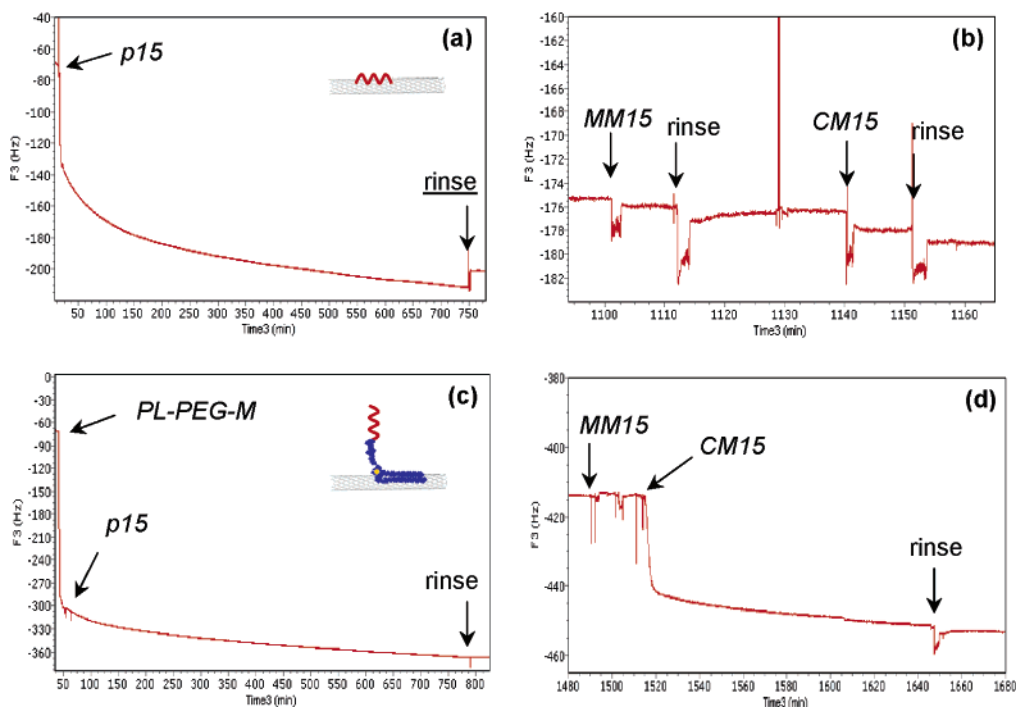


**Figure 2.** QCM frequency shift (F3) vs time curves showing that (a) thiolated 15mer ssDNA (*p15*) absorbs onto SWNT sidewall spontaneously and (b) no further binding to mismatched (*MM15*) and complementary (*CM15*) ssDNAs. (c) Phospholipid-PEG maleimide (*PL-PEG-M*) self-assembles onto SWNTs and allow effective linkage to *p15*. (d) The SWNT-*PL-PEG-M* linked ssDNA probes selectively hybridize to complementary strands. The inserts are schematic drawings of the SWNT-ssDNA complexes.

primarily by modulation of the contact resistance rather than the channel conductance.<sup>12</sup> The electrical measurement results shown by Star et al. can be better explained by contact work function change, rather than by doping. The lowering of p-type conductance was much more profound than the shift of conductance vs gate voltage ( $G-V_g$ ) curves. To clarify the sensing mechanism, we carried out XPS, QCM, and fluorescence measurements to evaluate ssDNA-SWNT binding and subsequent formation of double-stranded DNA (dsDNA) on SWNTs and gold surfaces separately. Our results suggest that the strong binding between the directly absorbed ssDNA molecules and the sidewalls of SWNTs largely inhibits further hybridization.

QCM measurements were done with a Q-sense D-300 instrument (Q-sense Inc) on optically polished quartz crystal substrates (5 MHz, AT cut) modified by drop dried chloroform suspended HipCo tubes. Frequency shifts due to mass uptake were measured at the third harmonic resonance of the crystal. Our data (Figure 2a) show that a significant amount of *p15* molecules (the same thiolated capturing ssDNA probe used in our electrical sensing experiment) bind to SWNT sidewalls irreversibly. The oscillation frequency shift of  $-140$  Hz at equilibrium corresponds to a probe density of  $\sim 4 \times 10^{13}$  molecules/cm<sup>2</sup>. After rinsing with PBS to remove free probes, relatively concentrated target ssDNA solutions  $1 \mu\text{M}$  *MM15* and *CM15* were introduced sequentially. No countable uptake was observed, which directly confirmed the lack of DNA hybridization on SWNT sidewall (Figure 2b). Control experiments were also done with nonthiolated *p15* to rule out the possible effect of thiolation. MCH treatment of SWNT-modified crystals does not incur

**Table 1.** XPS Quantifying Elemental Composition of SWNT Coated SiO<sub>2</sub> Surfaces after ssDNA (*p15*) Absorption and Subsequent Hybridization with Complementary Strand (*CM15*)<sup>a</sup>

substrate	% C	% N	% O	% P	% Si
SiO <sub>2</sub> , no tube, <i>p15</i>	5.27	0.57	62.68	<i>b</i>	31.32
SWNT on SiO <sub>2</sub> <i>p15</i>	8.97	0.9	60.52	0.14	29.46
<i>p15</i> + <i>CM15</i>	8.96	0.76	60.83	0.12	29.32

<sup>a</sup> Elevated carbon and nitrogen levels were observed as a result of DNA absorption. However, nitrogen is consistently present on all substrates due to contamination. Therefore, it cannot be used as a quantitative indicator of DNA on surface. <sup>b</sup> Not detectable.

any difference in QCM results. This result is consistent with our XPS data, as presented in Table 1, acquired on dense SWNT-matted SiO<sub>2</sub> substrates. The SWNTs synthesized here by iron nanoparticle catalyzed thermal CVD<sup>13</sup> closely resemble the characteristics of the tubes made for our sensing devices. All measurements were performed using a PHI Quantum 2000 scanning microprobe. Phosphorus (P) intensity was used as the signature to quantify surface absorption of oligonucleotides. There was no detectable P signal from SiO<sub>2</sub> (no tube) after soaking in  $10 \mu\text{M}$  *p15* solution overnight, indicating that thiolated ssDNA preferentially bonds to SWNTs instead of the hydrophilic SiO<sub>2</sub> surface. The *p15* anchored SWNT substrates further exposed to *CM15* solution for 2 h gave no change to P peak. Similar experiments were also done on Au surfaces (Table 2), where *p15* chemisorption on Au and subsequent hybridization with *CM15* were evident as expected. P is not detectable on the control sample soaked in buffer solution without DNA molecules. To obtain the same surface roughness and MCH coating as the sensor electrodes, the Au substrates were made by E-beam evapora-

**Table 2.** XPS Quantifying Elemental Composition of Au Surface after Thiol-ssDNA (*SH-p15*) Absorption and Subsequent Hybridization with Complementary Strand (*CM15*)

substrate	% C	% N	% O	% P	% Au
Au, buffer (no DNA)	27.50	2.89	24.18	<i>a</i>	40.94
SH-p15	36.15	7.60	28.91	1.71	22.79
SH-p15 + CM15	37.04	6.79	29.02	2.56	21.64

<sup>a</sup> Not detectable.

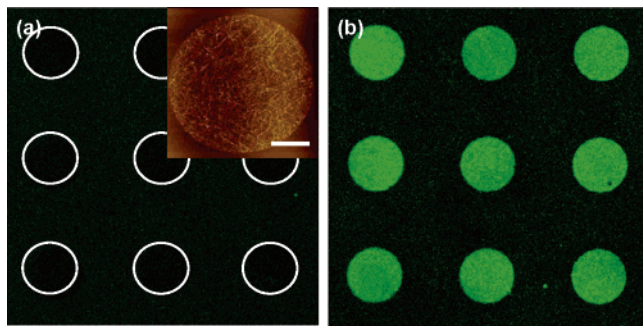


**Figure 3.** Fluorescence images showing DNA hybridization on patterned (circle) SWNT film. Thiolated ssDNA (probe) was conjugated to phospholipid–maleimide wrapped on a SWNT sidewall. Fluorescence intensity from cy3 labeled complementary target (b) is about five times higher than the mismatched (a). Insert is the atomic force microscopy image of one circle region (scale bar 5  $\mu\text{m}$ ).

tion of 30 nm gold layer onto  $\text{SiO}_2$  and then treated with MCH. These data suggest that thiol-modified ssDNAs (probes) immobilized on Au surface maintain their inherent affinity to their complementary strands, but not along the length of SWNTs, true to both drop-dried HipCo and CVD grown SWNTs despite their difference in tube diameter and film texture.

Theoretical modelings by Zheng et al.<sup>14</sup> and Gao et al.<sup>15</sup> suggest that a ssDNA molecule may wrap around a SWNT through  $\pi$ -stacking and van der Waals interaction. As a result, some DNA fragments could go through A–B conformation transition to reach a stable SWNT–DNA hybrid structure. Our observation is in perfect agreement with these theoretical predictions and the spectroscopy studies done by Dovbeshko et al.<sup>16</sup> and O’Connell et al.<sup>17</sup> The constriction of ssDNA

conformation on SWNT might have prevented or limited hybridization from occurring. To elucidate this phenomenon further, we designed a chemical scheme to reinstate the nanotube attached oligonucleotide functionality. Phospholipid-PEG maleimide (1,2-distearoyl-*sn*-glycero-3-phosphoethanolamine-*N*-[maleimide(poly(ethylene glycol)) 2000], Avanti Polar Lipids) molecules self-assembled on the sidewalls of SWNTs were used as the linker to immobilize ssDNAs and also as the spacer to block DNAs from directly stacking onto SWNTs. QCM data confirmed the effective covalent linkage of thiolated ssDNAs to the maleimide terminals on phospholipid-PEG (Figure 2c) and the selective hybridization of *p15* and *CM15* (Figure 2d), which was also evidently shown in the fluorescence images (Zeiss LSM 510 microscope) of substrates with patterned SWNT mats (Figure 3). The same scheme was employed to functionalize SWNT sensors for electrical measurements. Unfortunately, the enabled dsDNA formation along the tube length did not introduce detectable electrical response, due to possibly the relatively short Debye length in PBS ( $\sim 150 \text{ mM } [\text{Na}^+]$ ) compared to the long PEG chain and also blocking of the electrodes in close proximity of the tubes.

The pretreatment by MCH is believed to have a critical role in sensitizing and stabilizing our SWNT sensors in aqueous solution. DNA probe immobilization and hybridization on gold surfaces have been well studied in the past decade.<sup>18,19</sup> It is known that MCH forms a high-quality self-assembled monolayer (SAM) on gold. Our XPS analysis also revealed the preferential absorption of MCH on Au electrodes, but not on SWNTs (Supporting Information). The MCH SAM on Au electrodes provides a nice passivation against nonspecific binding (NSB) of mismatched ssDNA oligos and also an ideal probe orientation and density for efficient hybridization. Mixed monolayers of thiol-ssDNA and MCH on a gold surface exhibit nearly 100% binding efficiency toward analyte oligos carrying the complementary sequence.<sup>11</sup> Furthermore, MCH absorption on Au has an important effect on energy level alignment between the Au contact and SWNT.<sup>20</sup> The formation of MCH SAM on Au surface shifts the Au Fermi level toward the valence band of nanotubes and therefore decreases the carrier injection

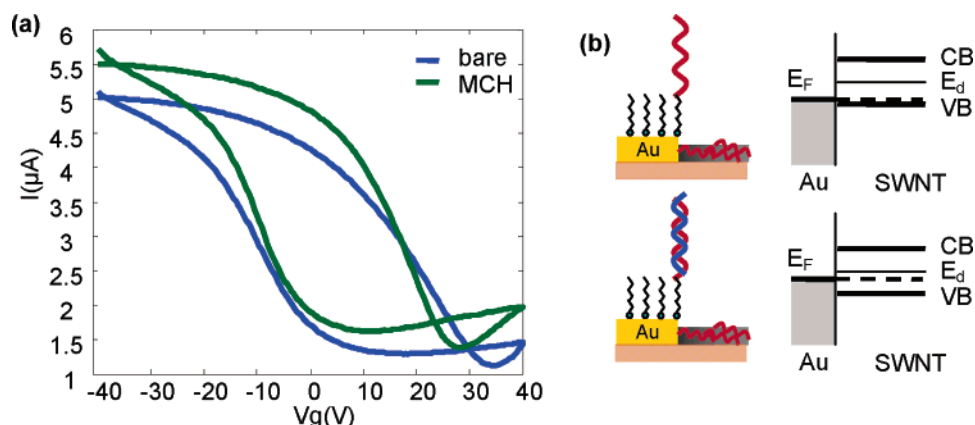


**Figure 4.** (a)  $I$ – $V_g$  curves taken by a sweeping silicon backgate showing the increment of device conductivity after MCH attachment to Au electrodes. (b) Schematic illustration of energy level alignment before and after DNA hybridization.

barrier. This is supported by the increased on-current observed in our electrical measurements (Figure 4).

We propose that the modulation of the Schottky barrier at the metal–tube contact by efficient hybridization on Au electrodes is the dominate sensing mechanism. The formation of dsDNA on gold electrodes lowered the effective work function of gold as illustrated in Figure 4. This is in total agreement with the scanning Kelvin probe studies reported by Hansen et al.<sup>21</sup> and Thompson et al.,<sup>22</sup> where formation of dsDNA reduced gold work function on the order of 0.01–0.1 eV (20mer to 40mer). Furthermore, the DNA hybridization kinetics observed real-time in our sensing experiments, consistent with that on gold surface, also strongly suggests that the electrical signal originates from hybridization events on the gold contact. Our QCM and XPS data conclude that the ssDNA probes wrapped on SWNTs played little role in hybridization; instead they blocked the NSB of analyte ssDNA oligos complementary or mismatched alike. The slight response to mismatched target DNAs is believed to be a combined result of the sequence-dependent DNA–SWNT affinity and the disruption of MCH and probe packing due to photoresist residues on the sensor surface.

In summary, we have developed fully electronic DNA sensors based on carbon nanotube field effect devices, which are readily scalable to high density sensor arrays and amenable to integration with “lab-on-a-chip” microanalysis systems. The generality of the sensors was demonstrated with synthetic oligonucleotides consisting of random generated sequences and also two different oligo lengths (15mer and 30mer). SWNT serves as the transducer which translates and amplifies DNA hybridization on Au into a directly detectable electrical signal. Compared to optical and other electrochemical methods, the essentially two-terminal SWNT DNA sensors involve much simpler chemistry and easier setup. A systematic investigation of sensing mechanism has provided us with great insights in SWNT–DNA interaction. The interference of DNA functionality by nanotube/DNA binding was addressed experimentally. Future direction will be toward small arrays with integrated microfluidic channels for sample preparation and delivery. On the other hand, it is highly desirable to fully utilize the surface and electrical properties of SWNT for biosensing in general, where chemical schemes for SWNT–biomolecule conjugation are in critical need that (1) preserve pristine nanotube property, (2) maintain biomolecule functionality, and (3) facilitate efficient SWNT–biomolecule charge transfer.

**Acknowledgment.** We thank Professor Hongjie Dai for his generous support and insightful discussions. This work was supported by the DARPA/MTO fund and a gift grant from Agilent Technologies.

**Supporting Information Available:** XPS data showing negligible absorption of MCH on SWNTs, and QCM data showing DNA probe immobilization and target hybridization on MCH-coated gold surface, which exhibits a kinetics consistent with our electrical measurements. This material is available free of charge via the Internet at <http://pubs.acs.org>.

## References

- (1) Wang, J. Portable Electrochemical Systems. *Trends Anal. Chem.* **2002**, *21*, 226–232.
- (2) Singhal, P.; Kuhr, W. G. Ultrasensitive Voltammetric Detection of Underivatized Oligonucleotides and DNA. *Anal. Chem.* **1997**, *69*, 4828–4832.
- (3) Wang, J. Carbon-Nanotube Based Electrochemical Biosensors: A review. *Electroanalysis* **2005**, *17*, 7–14.
- (4) Schoning, M. J.; Phoghossian, A. Recent Advances in Biologically Sensitive Field-Effect Transistors (BioFETs). *Analyst* **2002**, *127*, 1137–1151.
- (5) Pouthas, F.; Gentil, C.; Cote, D.; Bockelmann, U. DNA Detection on Transistor Arrays following Mutation-Specific Enzymatic Amplification. *Appl. Phys. Lett.* **2004**, *84*, 1594–1596.
- (6) Star, A.; Tu, E.; Niemann, J.; Gabriel, J. P.; Joiner, C. S.; Valcke, C. Label-Free Detection of DNA Hybridization Using Carbon Nanotube Network Field-Effect Transistors. *Proc. Natl. Acad. Sci. U.S.A.* **2006**, *104*, 921–926.
- (7) Hahm, J.; Lieber, C. Direct Ultrasensitive Electrical Detection of DNA and DNA Sequence Variations Using Nanowire Nanosensors. *Nano Lett.* **2004**, *4*, 51–54.
- (8) Qi, P.; Vermesh, O.; Grecu, M.; Javey, A.; Dai, H.; Peng, S.; Cho, K. J. Toward Large Arrays of Multiplex Functionalized Carbon Nanotube Sensors for Highly Sensitive and Selective Molecular Detection. *Nano Lett.* **2003**, *3*, 347–351.
- (9) Snow, E. S.; Perkins, F. K.; Houser, E. J.; Badescu, S. C.; Reinecke, T. L. Chemical Detection with a Single-Walled Carbon Nanotube Capacitor. *Science* **2005**, *307*, 1942–1945.
- (10) Chen, R. J.; Choi, H. C.; Bangsaruntip, S.; Yenilmez, E.; Tang, X.; Wang, Q.; Chang, Y.; Dai, H. J. An Investigation of the Mechanisms of Electronic Sensing of Protein Adsorption on Carbon Nanotube Devices. *J. Am. Chem. Soc.* **2004**, *126*, 1563–1568.
- (11) Peterson, A. W.; Heaton, R. J.; Georgiadis, R. M. The Effect of Surface Probe Density on DNA Hybridization. *Nucleic Acids Res.* **2001**, *29*, 5163–5168.
- (12) Heinze, S.; Tersoff, J.; Martel, R.; Derycke, V.; Appenzeller, J.; Avouris, Ph. Carbon Nanotubes as Schottky Barrier Transistors. *Phys. Rev. Lett.* **2002**, *89*, 106801.
- (13) Choi, H. C.; Kundaria, S.; Wang, D. W.; Javey, A.; Wang, Q.; Rolandi, M.; Dai, H. J. Efficient Formation of Iron Nanoparticle Catalysts on Silicon Oxide by Hydroxylamine for Carbon Nanotube Synthesis and Electronics. *Nano Lett.* **2003**, *3*, 157–161.
- (14) Zheng, M.; Jagota, A.; Semke, E. D.; Diner, B. A.; Mclean, R. S.; Lustig, S. R.; Richardson, R. E.; Tassi, N. G. DNA-Assisted Dispersion and Separation of Carbon Nanotubes. *Nat. Mater.* **2003**, *2*, 338–342.
- (15) Gao, H.; Kong, Y. Simulation of DNA-Nanotube Interactions. *Annu. Rev. Mater. Res.* **2004**, *34*, 123–150.
- (16) Dovbeshko, G. I.; Repnytska, O. P.; Obraztsova, E. D.; Shtogun, Y. V. DNA interaction with single-walled carbon nanotubes: a SEIRA study. *Chem. Phys. Lett.* **2003**, *372*, 432–437.
- (17) O’Connell, M. J.; Boul, P.; Ericson, L. M.; Huffman, C.; Wang, Y.; Haroz, E.; Kuper, C.; Tour, J.; Ausman, K. D.; Smalley, R. E. Reversible Water-Solubilization of Single-Walled Carbon Nanotubes by Polymer Wrapping. *Chem. Phys. Lett.* **2001**, *342*, 265–271.
- (18) Levicky, R.; Herne, T. M.; Tarlov, M. J.; Satija, S. K. Using Self-Assembly to Control the Structure of DNA Monolayers on Gold: A Neutron Reflectivity Study. *J. Am. Chem. Soc.* **1998**, *120*, 9787–9792.
- (19) Herne, T. M.; Tarlov, M. Characterization of DNA Probes Immobilized on Gold Surfaces. *J. Am. Chem. Soc.* **1997**, *119*, 8916–8920.
- (20) Cui, X.; Freitag, M.; Martel, R.; Louis, B.; Avouris, P. Controlling Energy-Level Alignments at Carbon Nanotube/Au Contacts. *Nano Lett.* **2003**, *3*, 783–787.
- (21) Hansen, D. C.; Hansen, K. M.; Ferrell T. L.; Thundat, T. Discerning Biomolecular Interactions Using Kelvin Probe Technology. *Langmuir* **2003**, *19*, 7514–7520.
- (22) Thompson, M.; Cheran, L.; Zhang, M.; Chacko, M.; Huo, H.; Sadeghi, S. Label-free Detection of Nucleic Acid and Protein Microarrays by Scanning Kelvin Nanoprobe. *Biosens. Bioelectron.* **2005**, *20*, 1470–1481.

NL060613V